Absorption of Sunlight in the Atmosphere of Venus

Abstract. *In this report the fluxes measured by the solar flux radiometer (LSFR) of the Pioneer Venus large probe are compared with calculations for model atmospheres. If the large particles of the middle and lower clouds are assumed to be sulfur, strong, short-wavelength absorption results in a net flux profile significantly different from the LSFR net flux measurements. Models in which the smallest particles are assumed to be sulfur gave flux profiles consistent with the measurements if an additional source of absorption is included in the upper cloud. The narrowband data from 0.590 to 0.665 micrometer indicate an absorption optical depth of about 0.05 below the cloud bottom. The broadband data imply that either this absorption extends over a considerable wavelength interval (as might be the case for dust) or that a very strong absorption band lies on one side of the narrowband filter (as suggested by early Venera 11 and Venera 12 reports). Thermal balance calculations based on the measured visible fluxes indicate high surface temperature for reasonable assumptions of cloud opacity and water vapor abundance. The lapse rate becomes convective within the middle cloud. For water mixing ratios of* 2.0×10^{-4} *below the clouds we find a subadiabatic region extending from the cloud bottom to altitudes near 35 kilometers.*

A brief description of the broadband upward, downward, and net flux of sunlight in the atmosphere of Venus measured by the solar flux radiometer (LSFR) on the Pioneer Venus mission was given in (*1*). Here we describe our first comparison of some of the measured net fluxes with model calculations. For this purpose, a trial cloud structure was adopted on the basis of the particle size distribution measurements of Knollenberg and Hunten (*2*). We have taken the number density of particles to be proportional to $r^{(1-3b)/b}e^{-(r/ab)}$, where r is the particle radius, a is the mean effective radius, and b is the mean effective variance [following Hansen (*3*)]. The total size distribution has been approximated by several size modes as shown in Table 1. We assumed that for each size mode, except mode 1 at pressures less than 0.183 atm, the particles were uniformly mixed with the gas in each pressure interval. We thought that the cloud particle size spectrometer (LCPS) data at lower pressures (down to the start of data at $\sim$ 0.12 atm) indicated a tendency for particle number density to decrease somewhat faster than the pressure for the mode 1 particles. We have assumed the scale height of the mode 1 particles to be half that of the gas at pressures less than 0.183 atm. It is of interest that in this model the cloud optical depth, τ, is 1.0 above the 50-mbar level and 0.15 above 10 mbar, both reasonable values (*4*).

One might expect the number of smaller (mode 1) particles to decrease more slowly with altitude than the larger (mode 2) particles, but if this were the case, the smaller particles would dominate the mode 2 particles at the $\tau = 1$ level, and probably be inconsistent with the ground-based polarization observations. The mode 2 particles, however, are of just the right size to be consistent with the polarization data if they dominate near the $\tau = 1$ level.

We emphasize that our present purpose is to adopt a rough working model for a first comparison with the LSFR flux measurements. Improved size distributions will surely be determined from the LCPS data (*5*), but we believe some interesting constraints on the composition of the various size modes can be obtained from even this preliminary model.

Because of their sizes, it seems reasonable to assume the mode 2 and 2′ particles are the H_2SO_4 particles deduced from ground-based observations. Here we examine in particular the hypothesis that the particles of mode 3 (and possibly also mode 1) are sulfur, as has been suggested by Knollenberg and Hunten (*2*). Figure 1 shows the net flux measured by the LSFR in the interval from 0.4 to 1.0 μm plotted against altitude compared with several models computed according to the layer-doubling and layer-adding method. Although the level of the net flux measurements depends sensitively on the calibration of the instrument, the shape of the curve with altitude should be well determined. Model I in Fig. 1 is the net flux computed for the case where the particles of both modes 1 and 3 are assumed to be sulfur, the absorption coefficient being taken from Young (*6*). As Young pointed out, models of this type with sulfur present over a wide range of temperatures are capable of reproducing the observed albedo of Venus in the ultraviolet region with no other sources of absorption. However, this model shows only a very slight decrease in the net flux in the upper cloud (where the data indicate a decrease of nearly 30 percent) and a decrease through the middle and lower cloud of some 26 percent where the data are relatively flat. We do not see any easy way to reconcile this model with our measurements.

If only the large (mode 3) particles are assumed to be sulfur, the model will not be dark enough to match the albedo of the planet at the shortest wavelengths. However, if the particles of mode 2 are allowed to have single-scattering albedos as low as 0.92 at short wavelengths because of impurities, this problem can be remedied. Model II is such a model with only mode 3 sulfur, the albedo of the mode 2 particles being artificially adjusted to match the ultraviolet albedo of Venus. This model has more absorption in the upper cloud than model I and very slightly less in the middle and lower cloud regions, but still looks very different compared to the data.

In model III it is assumed that only the small (mode 1) particles are sulfur. This time the albedo of the plant would be too high at intermediate wavelengths (0.45 to 0.50 μm) unless the single-scattering albedo of some other particles were decreased in this spectral region. If the albedo of the mode 2 particles is adjusted down to 0.99 at 0.47 μm, the albedo can be matched. The curve labeled model III in Fig. 1 has a shape that qualitatively matches the data through the cloud region. Although the levels of the curves for the data and the model are not quite the same, the present uncertainty in the level of the data is at least as great as this difference. Further, no attempt has been made to adjust the optical depths of the upper cloud above the region sampled by the LCPS beyond the simple extrapolation we have discussed. Thus, while refinements in both the LSFR calibration and the particle size distributions and optical depths deduced from the LCPS measurements may still be forthcoming, our data argue strongly against the possibility that the large (mode 3) particles of the middle or lower cloud can be sulfur (*7*).

In the region below the clouds, models I, II, and III all show a gentle rise due to the slight increase in the passband of our filters with increasing temperature. The data, on the other hand, show a significant decrease in the net flux in this interval. Constraints on the nature of this absorption can be gained by examining the LSFR narrowband data. The upward, downward, and net flux measured by the LSFR channel from 0.590 to 0.665 μm are shown in Fig. 2. Because the cloud optical properties can be assumed to change relatively slowly over this spectral bandpass, we can invert these fluxes for the single-scattering albedo and opti-

0036-8075/79/0706-0080$00.50/0

cal thickness of the atmosphere as a function of altitude if the single-scattering phase function of each atmospheric layer is known. We have done this for the model phase functions we determined from the LCPS data. In the cloud region, the optical depths resulting from the inversion of narrowband data are rather sensitive to a number of parameters (including the asymmetry parameter of the phase function used). However, below the clouds where the LCPS detected essentially no particles, we can safely use the Rayleigh phase function. In this region, the inversion of the narrowband LSFR data give scattering optical depths which agree with the Rayleigh scattering optical depths computed from the gas abundances to within about 5 percent. The single-scattering albedos derived imply an optical depth for absorption of about 0.045 in the region below the cloud in the spectral interval of the narrowband channels.

Since the narrowband data indicate the absorption of some 2 to 3 W/m² between the ground and the clouds, whereas the broadband data indicate the absorption of some 10 to 15 W/m², the absorption cannot be confined only to the wavelength interval of the narrowband. If the absorption is assumed to result from a very small number of dark "dust" particles having gray absorption below the clouds of model III, the broadband net flux profile would be that of model IV in Fig. 1, qualitatively similar in shape to the data.

Of course, it is possible that the absorption below the clouds seen in the narrowband channel is due to a very deep absorption that just overlaps either the short- or long-wavelength tail of the narrowband filter. In fact, the first reports of the results of the Soviet entry probes Venera 11 and Venera 12 indicate the presence of an unidentified strong absorption in the lower atmosphere at wavelengths shorter than about 0.55 μm. It will be interesting to compare their measurements with those from Pioneer Venus.

We have adopted an atmosphere having the structure of model III to compute the solar net flux profile from 0.3 to 4.0 μm, and have used this preliminary model to scale our solar flux measurements to planet-wide averages in order to estimate the influence of our data on globally averaged greenhouse models. We have adjusted the net flux at the top of the atmosphere to correspond to effective temperatures, T_E, between 230 K and 240 K. In the thermal infrared, mode 1 particles have negligible opacity, modes 2 and 2′ are assumed to be H_2SO_4, and mode 3 has been treated as a gray absorber with an opacity in the thermal infrared that is between 0.25 and 1.0 times the opacity of these particles at 0.6 μm. The gas opacity of CO_2 and H_2O are approximated following Pollack (*8*), and the water mixing ratio below the cloud is chosen between 2×10^{-4} and 2×10^{-3} decreasing ex-

Table 1. Preliminary model of cloud structure.

Mode	a (μm)	b	τ ≤ 0.183 atm	τ 0.183 to 0.321 atm	τ 0.321 to 0.960 atm	τ 0.960 to 1.32 atm
1	0.037*	10	4.23†	3.30	1.07	1.01
2	1.14	0.07	2.58	1.95	0	0
2′	1.65	0.0505	0	0	2.90	0.92
3	3.8	0.307	0	0	6.30	7.91
	Subtotal		6.81	5.25	10.27	9.84
	Total					32.17

*See (*11*). †See (*12*).

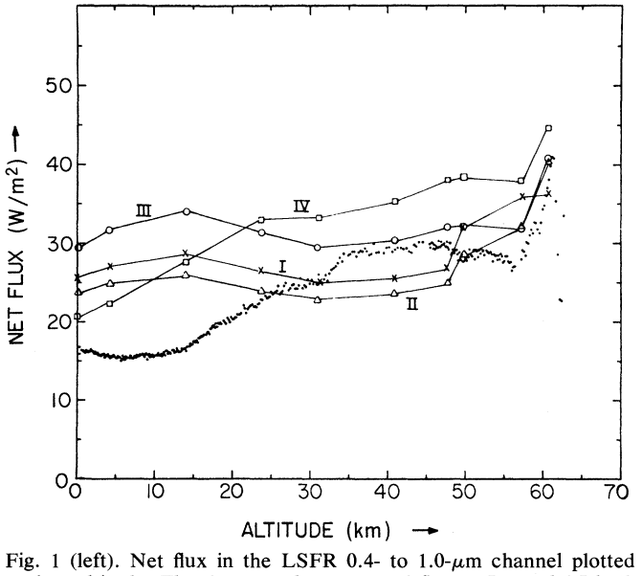

Fig. 1 (left). Net flux in the LSFR 0.4- to 1.0-μm channel plotted against altitude. The dots are the measured fluxes. In model I both mode 1 and mode 3 particles are assumed to be sulfur, which is the only absorber. It fails to fit the data in the upper cloud region (above 58 km). In model II only the mode 3 particles are sulfur, but an additional absorber is present in the upper cloud. Both models I and II fail to fit the data in the lower (47.5 to 50 km) and middle (50 to 57 km) cloud regions. In model III only the mode 1 particles are sulfur, and the absorber in the upper cloud is still present. Model IV is similar, but also has an optical depth of gray absorbing "dust" of 0.045 between the surface and 47.6-km altitude. The fluxes sometimes rise slightly toward lower altitudes because of broadening of the LSFR filter with temperature.

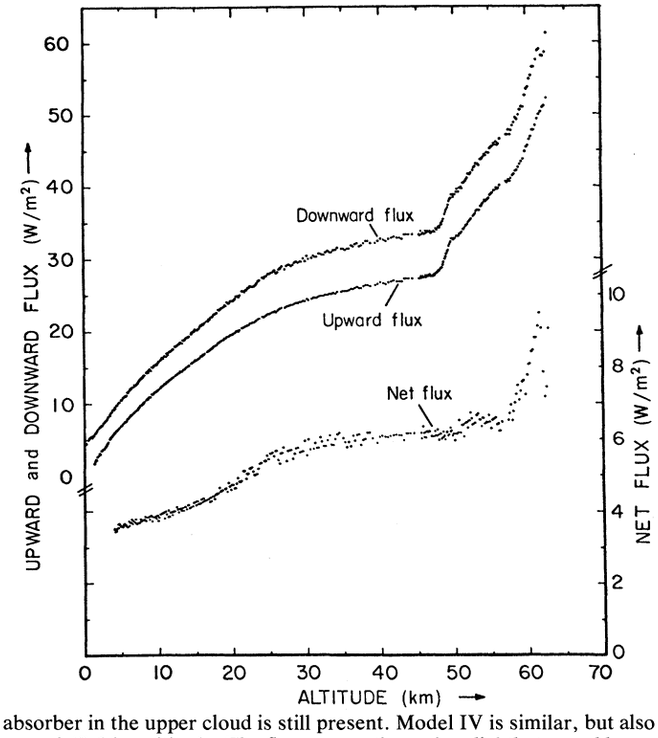

Fig. 2 (right). Upward, downward, and net flux in the 0.590- to 0.665-μm LSFR channel plotted against altitude. The drop in the net flux above 62 km seen in this figure and in Fig. 1 is thought to be caused by a horizontal inhomogeneity at the cloud tops.

ponentially with atmospheric pressure through the clouds to 10^{-6} above 57 km.

For T_E = 240 K, surface temperatures greater than 700 K are obtained even for our lowest opacity values. Lowering T_E to 230 K drops the surface temperature to as low as 675 K, but slight increases in cloud opacity or water mixing ratio easily bring it up to the measured value. The large cloud particles must have substantial opacity ($\gtrsim$ 0.25 times their opacity at 0.6 μm) in the window regions of the gas mixture for these high surface temperatures to be obtained.

The transition from radiative to convective equilibrium occurs in the middle cloud (50 to 57 km). For the low opacity case only the lower cloud is convective, and for high opacity both the middle and lower clouds can be convective. If the water abundance is low enough below the cloud bottoms, the CO_2 window regions create a subadiabatic layer beneath the clouds. The extent of this layer depends strongly on the water mixing ratio and for a value of 2×10^{-4} it extends to near 35 km before the atmosphere becomes opaque enough to become unstable again. It is interesting to note that Seiff *et al.* (*9*) find evidence for a subadiabatic region in this portion of the measured temperature profile.

If the large cloud particles have infrared-to-visible opacity ratios as large as 0.25, as Boese *et al.* (*10*) report, we conclude that it is relatively easy to obtain the measured high surface temperatures for reasonable water mixing ratios and a globally averaged net flux profile based on the LSFR data. For these cloud opacity ratios, there is always a convective region within the lower cloud deck. A subadiabatic region is also probable, but depends strongly on the exact water abundance and cloud opacity used in the model. Comparison of the measured temperature profile of Seiff *et al.* (*9*) suggests that our cloud bottom temperatures are generally on the low side if one accepts a cloud opacity ratio of 0.25. Increasing the net flux profile to the limit of the probable error bar, an increase of some 35 percent at this altitude, brings the profiles into better agreement.

MARTIN G. TOMASKO
LYN R. DOOSE, PETER H. SMITH
Lunar and Planetary Laboratory and *Optical Sciences Center, University of Arizona, Tucson 85721*

References and Notes

1. M. G. Tomasko, L. R. Doose, J. Palmer, A. Holmes, W. Wolfe, N. D. Castillo, P. H. Smith, *Science* **203**, 795 (1979).
2. R. G. Knollenberg and D. M. Hunten, *ibid.*, p. 792.
3. J. E. Hansen, *J. Atmos. Sci.* **28**, 1400 (1971).
4. L. D. Travis, D. L. Coffeen, J. E. Hansen, K. Kawabata, A. A. Lacis, W. A. Lane, S. S. Limaye, P. H. Stone, *Science* **203**, 781 (1979).
5. R. G. Knollenberg and D. M. Hunten, *ibid.* **205**, 70 (1979).
6. A. T. Young, *Icarus* **32**, 1 (1977).
7. At least for sulfur having properties described by the simplified expression in (*6*).
8. J. B. Pollack and R. Young, *J. Atm. Sci.* **32**, 1025 (1975); J. B. Pollack, *Icarus* **10**, 301 (1969); *ibid.*, p. 314.
9. A. Seiff *et al.*, *Science* **203**, 787 (1979).
10. R. W. Boese, J. B. Pollack, P. M. Silvaggio, *ibid.*, p. 797.
11. This size distribution was assumed to apply down to a lower limit of 0.1-μm radius, below which no particles were included.
12. The mode 1 particles in this region of the upper cloud have a gas-to-particle scale height ratio of 2. All other regions and modes are assumed to be uniformly mixed.
13. It gives us pleasure to acknowledge the support of N. Castillo and A. Holmes in data processing and instrument calibration.

15 May 1979

Preliminary Results of the Pioneer Venus Small Probe Net Flux Radiometer Experiment

Abstract. *Net radiation measurements in the atmosphere of Venus indicate that the bulk of the atmosphere is radiatively cooling at high latitudes and heating at low latitudes. Similarity of features observed by all three probes indicate planetwide stratification. Flux variations within the clouds provide evidence of significant differences in cloud structure. A feature of unusually large opacity found near 60 kilometers at the north probe site is probably related to the unique circulation regime revealed by ultraviolet and infrared imagery. A stable layer between the cloud bottoms and about 35 kilometers contains several features in the flux profiles probably resulting from large-scale compositional stratifications rather than clouds. In the layer below 35 kilometers unexpectedly large fluxes were observed.*

A small probe net flux radiometer (SNFR) was flown on the north, day, and night probes of the Pioneer Venus mission, sampling the atmosphere over a wide range of latitudes and longitudes (*1*). All three instruments operated successfully from deployment down to an altitude of 12.5 km (*2*), measuring the total planar net flux density (termed net flux herein) as a function of altitude. Since the divergence of the net flux equals the radiative power input per unit volume, the altitude derivative of the SNFR measurements directly defines the vertical distribution of radiative energy sources and sinks which power the atmospheric circulations. Also embodied in the SNFR data is information about the opacity structure of the atmosphere; the measured flux profiles place constraints on the sources of opacity—the gases and particulates through which radiative transfer takes place. The preliminary results of this experiment are presented here, following a short description of the instrument measurement characteristics.

The SNFR measures the difference between upward and downward fluxes directly by means of an external sensor with a wide field of view deployed beyond the edge of the probe's heat shield. The sensor consists of a thermopile-equipped flux plate protected by a pair of diamond windows. A heater is incorporated to prevent condensation and to minimize errors produced by a sensor thermal lag relative to the atmosphere. A sensor temperature monitor provides data needed to correct for a temperature-dependent responsivity. The radiation field is mechanically chopped by flipping the sensor at a 1-Hz rate, thereby canceling thermal and electrical offsets generated by the environmental extremes experienced in descent. Further instrumentation details can be found in (*3*).

The SNFR flux measurements spectrally integrate radiation in a wide bandpass from ultraviolet to far infrared with nearly uniform weighting at all wavelengths where significant net flux is possible within the atmosphere (Fig. 1). At the north and night probe sites, where solar radiation was absent, the SNFR measured only planetary radiation. The day probe SNFR measured the sum of the net planetary and net solar fluxes. The angular response of the SNFR, when averaged over a complete probe rotation, approaches the cosine response of an ideal flat plate (Fig. 2). The error in the SNFR fluxes due to angular and spectral response defects is estimated to be less than 1 percent on the basis of simulations performed with an infrared radiative transfer model (*4*).

The net flux measurements from all three probes are shown in Fig. 3 with positive values indicating net upward flux. Note that the solar contribution to the day probe net flux makes the total smaller than observed at the other sites. The altitude scale is based on data from the small probe atmospheric structure (SAS) experiment (*5*). To facilitate direct intercomparisons with other experiments, ground receipt time for each probe is shown on inserted scales. All of the data obtained prior to and immedi-

0036-8075/79/0706-0082$00.50/0